Received: 20 December 2020 | Revised: 6 February 2021 | Accepted: 17 February 2021
DOI: 10.1002/hyp.14102

RESEARCH ARTICLE

WILEY

# Effects of pipe outlet blocking on hydrological functioning in a degraded blanket peatland

Taco H. Regensburg[1] | Pippa J. Chapman[1] | Michael G. Pilkington[2] | David M. Chandler[2] | Martin G. Evans[3] | Joseph Holden[1]

[1]School of Geography, University of Leeds, Leeds, UK

[2]Moors for the Future Partnership, The Moorland Centre, Edale, UK

[3]School of Environment, Education, and Development, The University of Manchester, Manchester, UK

**Correspondence**
Taco H. Regensburg, School of Geography, University of Leeds, Leeds LS2 9JT, UK.
Email: gytr@leeds.ac.uk

**Funding information**
Moors for the Future Partnership, Grant/Award Number: EU-MoorLife2020-D3

## Abstract

Peatland restoration practitioners are keen to understand the role of drainage via natural soil pipes, especially where erosion has released large quantities of fluvial carbon in stream waters. However, little is known about pipe-to-stream connectivity and whether blocking methods used to impede flow in open ditch networks and gullies also work on pipe networks. Two streams in a heavily degraded blanket bog (southern Pennines, UK) were used to assess whether impeding drainage from pipe networks alters the streamflow responses to storm events, and how such intervention affects the hydrological functioning of the pipe network and the surrounding peat. Pipeflow was impeded in half of the pipe outlets in one stream, either by inserting a plug-like structure in the pipe-end or by the insertion of a vertical screen at the pipe outlet perpendicular to the direction of the predicted pipe course. Statistical response variable $\eta^2$ showed the overall effects of pipe outlet blocking on stream responses were small with $\eta^2 = 0.022$ for total storm runoff, $\eta^2 = 0.097$ for peak discharge, $\eta^2 = 0.014$ for peak lag, and $\eta^2 = 0.207$ for response index. Both trialled blocking methods either led to new pipe outlets appearing or seepage occurring around blocks within 90 days of blocking. Discharge from four individual pipe outlets was monitored for 17 months before blocking and contributed 11.3% of streamflow. Pipe outlets on streambanks with headward retreat produced significantly larger peak flows and storm contributions to streamflow compared to pipe outlets that issued onto straight streambank sections. We found a distinctive distance-decay effect of the water table around pipe outlets, with deeper water tables around pipe outlets that issued onto straight streambanks sections. We suggest that impeding pipeflow at pipe outlets would exacerbate pipe development in the gully edge zone, and propose that future pipe blocking efforts in peatlands prioritize increasing the residence time of pipe water by forming surface storage higher up the pipe network.

**KEYWORDS**
discharge, hydrological connectivity, pipeflow, restoration, water table, wetland

# 1 | INTRODUCTION

Soil piping has been reported in all regions of the world (Bernatek-Jakiel & Poesen, 2018), but most commonly in tropical forests (Chappell, 2010), loess soils (Verachtert et al., 2010; Zhu et al., 2002), subarctic hillslopes (Carey & Woo, 2002), dispersive semi-arid soils (Faulkner, 2013), boreal forests (Roberge & Plamondon, 1987), steep temperate hillslopes (A. E. Anderson et al., 2009), and peatlands (M. Anderson & Burt, 1982; Rapson et al., 2006). Pipes can act as important hydrological and geomorphological agents (Bryan & Yair, 1982; Gilman & Newson, 1980; Jones, 1971). Soil piping is increasingly recognized as a significant factor in soil degradation in many natural and anthropogenic landscapes (Bernatek-Jakiel & Poesen, 2018). Pipes often erode to form gullies (Wilson, 2011; X. Xu et al., 2020) and can be a common feature of degraded landscapes. Piping has been widely reported in British upland regions (e.g., Jones et al., 1997), and is particularly prevalent in sloping blanket peat (Holden, 2005). Peatlands are important global carbon stores and in some regions, including the British Isles, are source areas for significant proportions of potable water (J. Xu et al., 2018). Headwater peatlands can often also be source areas for flooding (Acreman & Holden, 2013). Given these ecosystem service drivers, there has been increasing attention paid to the degraded state of some headwater peatlands and whether active management of pipe networks and pipeflows in peatlands might be important for managers to consider as part of peatland restoration projects.

Peatlands cover around 10% of the British Isles but many of these have been subject to damage from peat abstraction, drainage, overgrazing, burning and atmospheric pollution (Evans & Warburton, 2007; S. M. Smart et al., 2010; Ward et al., 2007). In the southern Pennines of England, widespread peat erosion is most commonly ascribed to atmospheric deposition of acidic pollutants which, since the Industrial Revolution, has severely damaged peat forming mosses (Yeloff et al., 2006). The erosion is severe including much gullying (Evans et al., 2006), and causes problems downstream including reservoir sedimentation (Labadz et al., 1991) and enhanced water discolouration, increasing treatment costs for potable supplies (Bonn et al., 2010; Fearing et al., 2004; Van der Wal et al., 2011). In that context, downstream flooding is a major concern and recent work has suggested that peatland restoration could contribute to reduced flood peaks and delayed peak flow times through slowing flow accumulation in headwaters (Gao et al., 2016; Grayson et al., 2010; Holden et al., 2008; Shuttleworth et al., 2019).

Pipe outlets are observed at the head and on banks of gullies in degraded blanket peatlands (Regensburg et al., 2020). The role of pipeflow in flood generation from peatlands remains unclear, but pipeflow can be an important contributor to flow in peatland streams (e.g., Chapman, 1994; Chapman et al., 1993, 1997; Gilman & Newson, 1980; Holden & Burt, 2002; Jones, 1982; Jones, 1997a; Jones & Crane, 1984; R. P. Smart et al., 2013). For a histic podzol system in Wales, Jones (1997b) reported pipes to respond at different times during the same storm event and these lag times varied between events, depending on antecedent wetness and rainfall intensity. However, there is a lack of pipeflow studies in heavily degraded peatland systems where water tables can be deep adjacent to gullies (Daniels et al., 2008) and interactions between water tables and pipeflow in peatlands are not well studied.

Keeping peatlands saturated is an important target of restoration work since shallow water tables are required to reduce peat decomposition and maintain net C uptake. Gully banks are accessible to practitioners who are keen to know whether impeding flow at pipe outlets on gully banks is a viable component of peatland restoration. Plugging of pipe outlets in mineral soils showed soil pore saturation to increase upslope of the plugs (Wilson & Fox, 2013), and it was hypothesized that with time after pipe plugging new pipes may form (Midgley et al., 2013). Frankl et al. (2016) showed impediment of subsurface flows by use of geomembranes perpendicular to the flow direction could increase wetness of areas upslope of the subsurface screen and stabilize gully heads, but downstream impacts of impeding pipeflow have not been studied. Here we report on an experiment investigating the impact of pipe outlet blocking on streamflow in a heavily degraded blanket bog. This paper aims to:

1. investigate whether impeding pipeflow at pipe outlets in degraded blanket peat alters the stormflow response of streams, and
2. explore how pipe outlet blocking affects the hydrological functioning of soil pipes and the water table in the surrounding peat.

# 2 | STUDY SITE AND EXPERIMENTAL DESIGN

## 2.1 | Field area

The study was conducted in the Upper North Grain (UNG) catchment on the southern flank of the Bleaklow plateau in the Peak District National Park in northern England. The system drains an area of 0.49 km$^2$ and enters the Ashop, a river flowing in southeastly direction (Figure 1a). The catchment has an altitudinal range of 467–540 m and a south–south-west aspect (Figure 1b). The site has a sub-Arctic oceanic climate with a mean annual temperature of 6.9°C and an annual precipitation of 1313 mm (2004–2013) (Clay & Evans, 2017). The pedology of UNG is characterized by blanket peat, being 4 m thick in places, with an active vegetation layer consisting of *Eriophorum vaginatum*, *Eriophorum augustifolium*, *Calluna vulgaris*, *Erica tetralix*, *Vaccinium myrtillus*, *Empetrum nigrum* and patches of *Sphagnum spp*. Peat is deposited on a thin, discontinuous periglacial head deposit covering solid sandstones of the carboniferous age Millstone Grit Series (Wolverson Cope, 1998). Slopes in the catchment vary between 0° and 15°, with the majority of the catchment (>80%) being between 0° and 7°. The peat cover on UNG is regarded as degraded and characterized by an extensive network of deep gullies which, in the lower reaches, cut into the underlying bedrock. Further details on the erosion history of the catchment can be found in Regensburg et al. (2020). They found 346 pipe outlets throughout the UNG catchment, and linked their occurrence to desiccation processes in straight streambank sections ("edge location"), and places where headward erosion occurred around the pipe outlet ("head location"). Unless differences between pipe outlets at these two

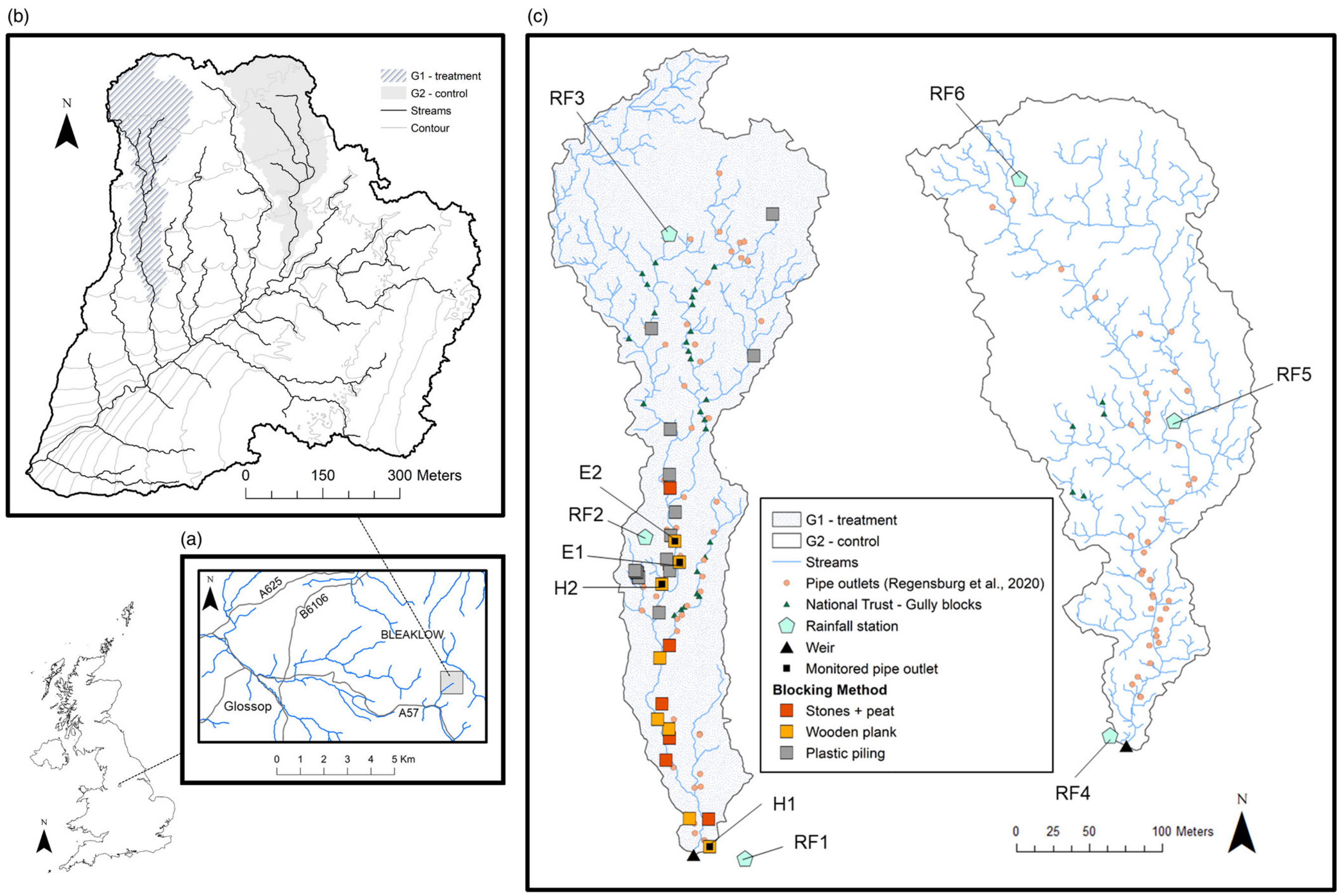


**FIGURE 1** (a) Location of Upper North Grain study catchment; (b) the location of the selected sub-catchments in the stream network, with contour intervals of 5 m from 535 to 480 m above sea level; (c) monitoring setup for the sub-catchments showing the location of pipeflow gauges at head locations (pipe H1 and pipe H2) and edge locations (pipe E1 and pipe E2), rainfall stations (RF1 – 6), and weirs (black large triangle) at catchment outlets. Materials used to block pipe outlets: 1. Mixture of peat and stones (red), 2. Wooden plank (orange), and 3. Plastic pilling (grey). Identified pipe outlets in both catchments (beige circles) are added for reference. Note that the area of tributaries affected by gully blocks (small triangles – Green) is larger for the treatment catchment compared to the control catchment

locations are discussed, hereafter, further references to the identity of pipes with outlets at these two locations will be made by using the terms "edge pipes" or "head pipes" respectively. The majority of pipe outlets were observed in the upper meter of the peat deposit (Regensburg et al., 2020). As part of ongoing peatland restoration works in the area, the National Trust had carried out gully blocking in a number of tributaries at UNG between 2013 and April 2018 which consisted of: (1) placing tree trunks in the streambed (2013) on the southern flanks of the catchment, and (2) wooden planks and stone boulders (2018) in the northern flanks of the catchment (Figure 1c). All gully blocks were installed before monitoring of stream- and pipeflow commenced.

## 2.2 | Experimental design

To determine the impact of impeding pipeflow on streamflow, a before-after-control-intervention (BACI) study design was implemented, comparing hydrological responses of two sub-catchments before and after pipe outlets were blocked in one of them. The two sub-catchments, "Control" and "Treatment", were selected based on comparable geometry, orientation and frequency of pipe outlets (Regensburg et al., 2020), using DEMs (0.5 m resolution LiDAR) and field verification (Table 1, Figure 1b).

The experiment commenced in April 2018, and covered a pre-blocking period of 17 months ("pre"), and a post-blocking period of 6 months (September 2019–February 2020) ("post"). In the treatment catchment, pipe outlets were blocked in autumn 2019, whereas pipe outlets in the control site were left unaltered. Pipeflow was ephemeral and responses to storm events were studied by monitoring pipe discharge and water-table depth at four pipe outlets in the intervention catchment, which all had a mean outlet diameter larger than 10 cm. Two pipes were monitored at head locations (pipe H1 and pipe H2), and two pipes monitored at edge locations (pipe E1 and pipe E2) (Figure 1c).

## 2.3 | Pipe outlet blocking

Pipe outlets were blocked using two methods: (1) the insertion of a plug-like structure in the pipe-end, and (2) the insertion of a vertical screen at the pipe outlet perpendicular to the direction of the predicted pipe course. Materials used involved jute bags filled with peat, a mixture of peat and stones, wooden planks, and plastic pilling (Figure 3), within practical labour costs and sustainable resource use constraints. Plugging pipe outlets with on-site available materials was considered to be less destructive to the peat and would only affect the direct surroundings of a pipe outlet, whereas screens would form an impermeable barrier to both pipe water and throughflow of the surrounding peat. Therefore, prior to field trials, a laboratory test was performed to investigate the sealing strength of peat as a blocking medium (for design see Appendix A in Data S1, Figure S1). Results showed that peat plugs sealed themselves under a constant pressure head. To verify whether a similar result could be achieved in situ, blocking trials were carried out at UNG on four pipe outlets that were not within either of the two monitored sub-catchments, between May and August 2019. The first attempts involved constructing a plug-like structure consisting of a jute bag filled with locally sourced peat (Figure 2a), which was inserted up to 30 cm into the pipe outlet. Time-lapse cameras captured any surface changes of the newly blocked pipe outlets and any seepage of water over a 2 week period after blocking. The footage showed water was observed emanating either side of the plug. In a second attempt, the same outlets were filled over the same length with a mixture of peat and stones, sourced from the nearest stream bed (Figure 2b), which resulted in a more

**TABLE 1** Details of the two sub-catchments monitored in Upper North Grain

| | Control catchment | Treatment catchment |
|---|---|---|
| Catchment outlet | 53°26′31″ N, 001°50′16″ W | 53°26′28″ N, 001°50′30″ W |
| Elevation of outlet (m asl) | 519.1 | 511.8 |
| Area (m$^2$) | 43 178 | 37 506 |
| Mean slope (°) | 6.11 | 7.68 |
| Flow direction of main channel | south west to south east | south |
| Number of pipe outlets[a] | 41 (5 head; 39 edge) | 65 (25 head; 40 edge) |
| Number of blocked pipe outlets | 0 | 31 |

[a]Identified in 2018–2019 pipe outlet survey (Regensburg, 2020).

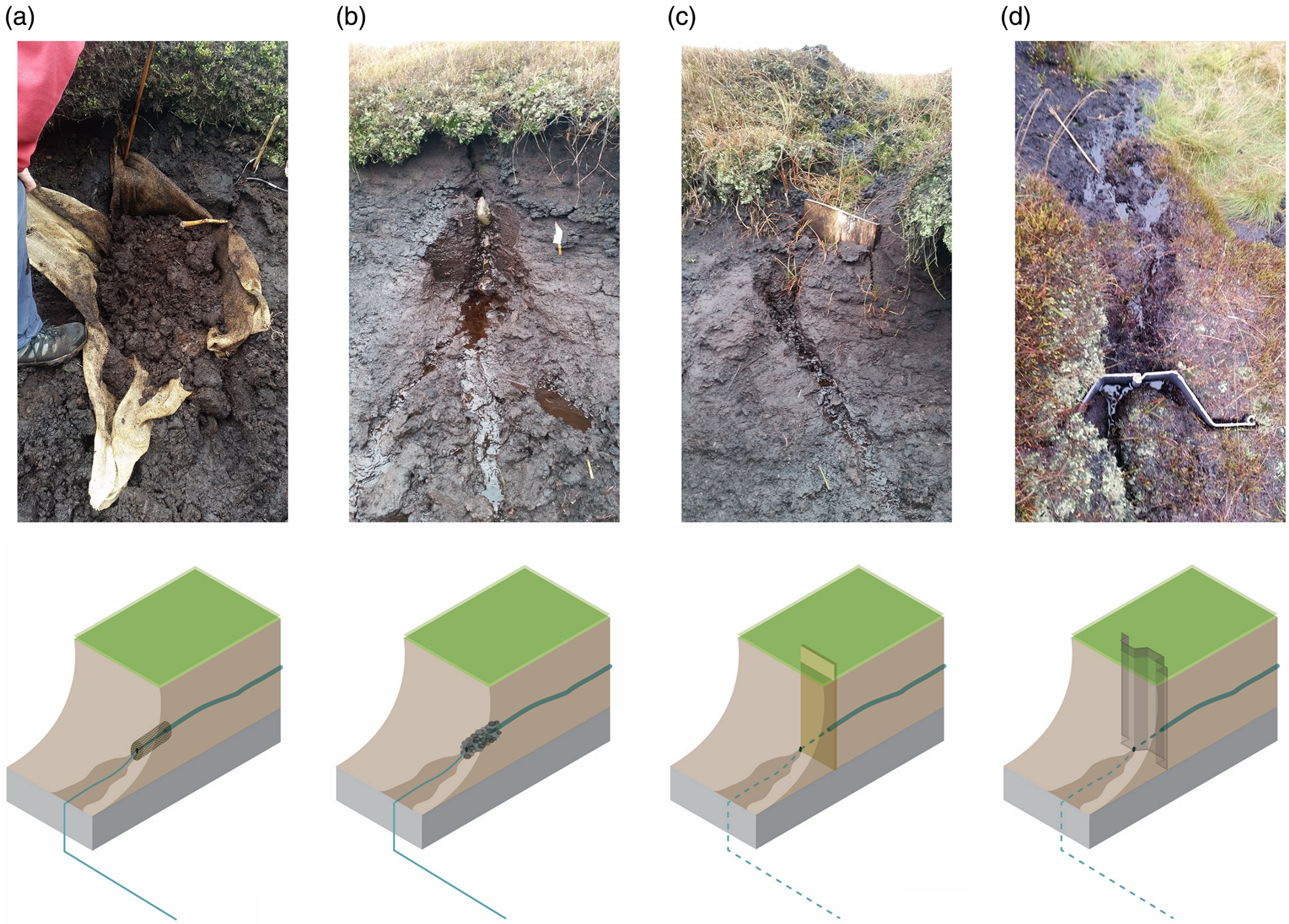


**FIGURE 2** Schematic showing the design and in-field application of plug-like structures and vertical screens to block pipe outlets: (a) jute bag filled with peat, (b) mixture of peat and stones, (c) wooden plank, and (d) plastic pilling. Illustrations produced by P.T.J Lewis

varied seepage pattern, with at least one blocked pipe outlet being occasionally dry while others still showed active seepage around the plug.

Between 20 August and 24 September 2019, pipe outlets with clear evidence of recent pipeflow were blocked in the treatment catchment. Initially, 10 pipe outlets were blocked by inserting a plug-like structure involving a mixture of peat and stones, but water was observed percolating around and through all of them within 7 days of blocking. Therefore, further blocking focused on the insertion of vertical screens of marine plywood ("wooden planks") (Figure 2c) and later plastic pilling (Figure 2d). Screen widths ranged between 0.3 and 1 m. The four pipe outlets with a pipeflow gauge were each blocked with a wooden plank of 1 m width, which was inserted up to at least twice the depth of the pipe outlet relative to the peat surface. Where feasible, pipe outlets initially blocked with a mixture of peat and stones received either a wooden or a plastic screen. By 24 September 2019, a total of 31 pipe outlets had been blocked in the treatment catchment resulting in six blocks with a mixture of peat and stones, eight with wooden planks, and 17 with plastic pilling. These 31 blocked outlets represented 68% of the total identified pipe outlets across the treatment catchment at that time (Regensburg, 2020). On 27 September 2019 a further 20 pipe outlets were identified in two tributaries of the treatment catchment, which both had gully blocks in them (Regensburg, 2020). Between August 2019 and February 2020, the 31 blocked pipe outlets in the treatment catchment were assessed for leakiness through the observation of seepage from photos taken at biweekly intervals. When seepage was observed, its most dominant flow route was determined using the following classification: (1) unidentifiable, (2) from the old outlet only, (3) from new outlets only, and (4) a combination of old and new outlets. For each observation of seepage the rate of flow was visually estimated, using pipe discharge measurements before blocking (see below).

## 3 | MONITORING

### 3.1 | Precipitation

Rainfall stations were installed at three locations within each subcatchment, equidistantly spaced between the stream outlet and the head of the respective stream network. Each rainfall station comprised of a tipping bucket (DAVIS AeroCone with 0.2 mm resolution) recording at 5-min intervals, and a storage gauge to measure accumulated rainfall between field visits (approximately every 2 weeks). One rainfall station (RF2) was placed next to pipe E2 in April 2018, with the other five being installed in December 2018 (Figure 1c).

### 3.2 | Stream discharge

Stream discharge was gauged at the outlet of each catchment by insertion of a weir plate using a calibrated V-notch. Water head above the notch was recorded using a vented pressure transducer (In-Situ Troll 500) that was placed in a stilling well ~1 m upstream of the weir crest. Stage was recorded at 5-min intervals. At low flows, up to 0.5 litre per second, a stage discharge relationship was determined by measuring the volume of water per unit of time using a measuring cylinder and stopwatch. At higher flows, salt dilution gauging was carried out in a 10 m straight section downstream of the weir. A stage-discharge relationship for each stream was constructed by combining the results from the two methods. Streamflow monitoring

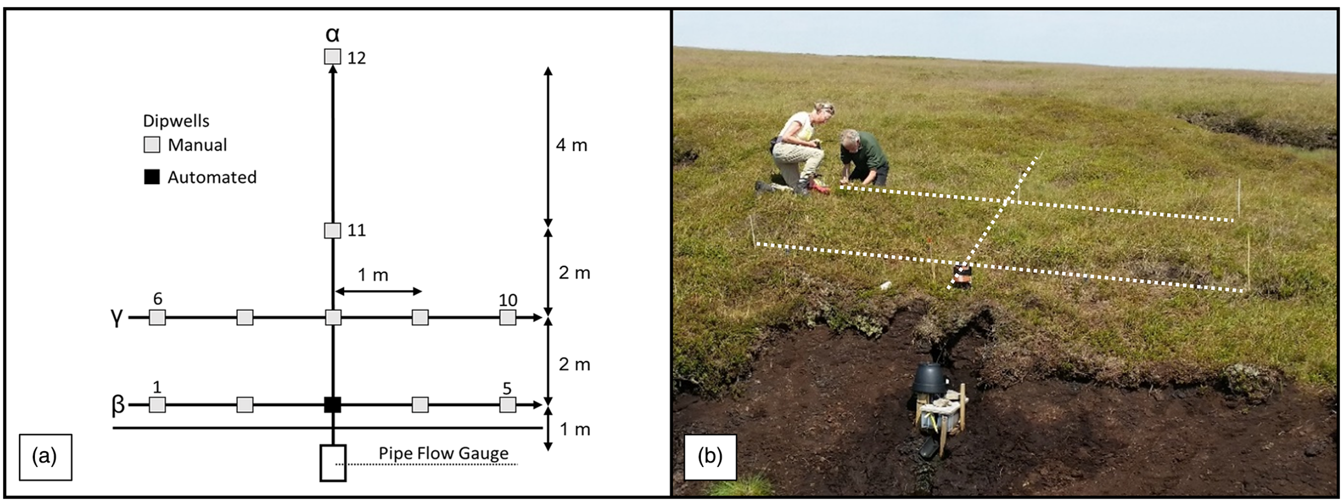


**FIGURE 3** Monitoring of water table at each gauged pipe outlet location: (a) schematic of dipwell set up around gauged pipe outlets. Dipwells were placed along transect lines α, β, and γ. Transect lines β and γ were used to characterize the lateral water table interactions from the projected pipe course, and α to determine water table parallel to the projected pipe course. Transect β and γ run parallel to the gully edge; (b) volunteers measuring water-table depth at pipe E1 on 16 July 2019. White dotted lines indicate the approximate position of the dipwell transects (β and γ parallel to gully edge, and α perpendicular to it)

commenced in October 2018 for the treatment catchment and in December 2018 for the control catchment.

### 3.3 | Pipe discharge

Pipe discharge was monitored at four pipe outlets in the treatment catchment: pipe H1 (May 2018 to February 2020), pipe H2 (May 2018 to December 2019), pipe E1 (October 2018 to August 2019), and pipe E2 (May 2018 to February 2020). At each pipe outlet, water was channelled via guttering into a rectangular plastic box of 140 mm × 340 mm × 220 mm with a 22.5° V-shaped opening, hereafter referred to as "pipeflow gauge". Each pipeflow gauge was instrumented with a vented pressure transducer (In-Situ Troll 500), which recorded water level above the sensor head in the box at a 5-min interval. Gutters from the pipe outlet to the pipeflow gauge were shielded from rainfall using waterproof tape or polyethylene plastic sheeting. After blocking pipe outlets in August 2019, any water that appeared around or close to the blocked outlets that were monitored, was redirected to the respective pipeflow gauge, where possible, using guttering, to quantify the amount of water escaping from the blocked pipe. During field visits, when water was flowing over the notch of the V, discharge from the pipeflow gauges was measured using a measuring cylinder and a stopwatch, to derive a stage-discharge relation. The seepage around other blocked pipe outlets observed during field visits was visually estimated as No Flow, Low (<0.05 L $s^{-1}$), Medium (0.05–0.50 L $s^{-1}$), and High (>0.5 L $s^{-1}$).

### 3.4 | Water-table depth

Water table was measured around each of the four pipe outlets, using a network of 12 dipwells, that was set up in three transects, of which one was parallel to the projected pipe course (α) and two perpendicular to it (β and γ). Transect α had four dipwells at 1, 3, 5 and 9 m from the pipe outlet (Figure 3a). Transects β and γ each had five dipwells spaced equidistantly every 1 m with the middle dipwell on transect α, at 1 and 3 m from the pipe outlet respectively (Figure 3a). Each dipwell comprised a 1 m length of polypropylene pipe (internal diameter 30 mm) with perforations at 50 mm intervals, with four holes at a 90° spacing per interval. Dipwells were driven into pre-prepared boreholes. A removable cap was placed on top of each dipwell to prevent water ingress by rainfall or animal disturbance (Figure 3b). The dipwell closest to the pipe outlet was instrumented with an automated water-level logger (In-situ Troll 500), recording at 5-min intervals. At the other 11 dipwells, water-table depth was measured manually every 2 weeks by inserting a sounding dip-meter. Continuous water-table records for the automated dipwells were available for all four pipe locations, but spanning different periods: pipe H1 May 2018 – January 2020, pipe H2 May 2018 – December 2019, pipe E1 May 2018–December 2019, and pipe E2 May 2018 – December 2019. Between April and August 2019 water-table data were not available for pipe H2 and pipe E1 due to equipment failure.

## 4 | DATA PROCESSING

Operational issues led to occasional periods where no data were available for some locations.

### 4.1 | Precipitation

Gaps in rainfall timeseries were referenced to nearby stations (for details see Appendix B in Data S1). An antecedent precipitation index (API) was derived for the catchment preceding storm events using a universal API equation after Kohler and Linsley (1951):

$$API_t = API_{t-1}\,k + P_{\Delta t}, \tag{1}$$

where $API_t$ is API at time t, $P_{\Delta t}$ is the precipitation occurring between times t−1 and t, and $k$ is the recession coefficient. API was calculated for a period of three consecutive days prior to each storm event, using daily precipitation totals for $P_{\Delta t}$. In this study a value of 0.5 was chosen for $k$.

### 4.2 | Storm responses

Hydrological responses were derived from rainfall time series from April 2018 to February 2020, at time steps of 5 min. Stream and pipe discharge series were screened for responses to rainfall events in excess of 1 mm over at least three consecutive time steps. A total of 141 storms were identified, covering 93 events in the pre-blocking period and 48 events post-blocking. The response of stream- and pipeflow to each individual storm was quantified as long as the following criteria were met:

1. The event was rainfall-driven and not associated with snowmelt.
2. Storm responses were single peaked, but minor secondary peaks with peak discharge of less than 20% of the total storm peak discharge were allowed to help achieve temporal representativeness across stream- and pipeflow.
3. Storm responses were not included when data gaps occurred around the projected discharge peak.

This resulted in different numbers of hydrographs being analysed for pre- and post-blocking at each catchment and pipe outlet (Table 2).

Hydrograph response was quantified using four metrics: (1) storm discharge – the total volume (in mm or L) of water leaving the weir during an event; (2) peak lag – the time (in hours) between peak rainfall and peak discharge; (3) peak discharge – the highest discharge (L $s^{-1}$) reached during the storm; (4) duration of storm discharge – the total time for which the measured discharge was larger than baseflow (Figure S2). To account for the impact of catchment area on stream discharge, storm discharge was divided by topographic drainage area, providing specific discharge, expressed in mm; the runoff coefficient was also calculated as a function of total storm rainfall. Because the topographic drainage area of pipe outlets is not known, a theoretical dynamic contributing area was calculated by dividing total pipe discharge by total rainfall, assuming a rainfall-to-runoff conversion of 100%. To characterize hydrograph shape, a response index was calculated by dividing storm peak discharge by the time duration that storm discharge was larger than baseflow. For events with peak discharges outside the confidence window of the stage-discharge curves, the raw stage data of each respective sensor was used to determine the time of peak discharge. Recession rates for water table were derived from the gauged dipwell closest to each pipe outlet, and calculated as a mean over 6 and 12 h after rainfall cessation (Figure S2).

Most variables did not follow a normal distribution, therefore non-parametric tests of difference were employed. When groups of data violated assumptions for homogeneity of variance, differences between groups were explained in terms of their distributions, otherwise median differences were reported. The combined effect of blocking 31 individual pipe outlets on streamflow was determined by calculating a statistical response variable ($\eta^2$) for storm events to which both sub-catchments responded. For metrics depending on peak discharge, data were normalized for each stream to values between 0 and 1 before subtracting control from treatment data. Data on runoff coefficients and peak lag were both ratio data, therefore scaling was not applied, and difference was calculated by subtracting control from treatment. The statistical response variable was calculated as follows:

$$\eta^2 = \frac{Z^2}{n-1}, \tag{2}$$

where Z is the standardized test statistic in the Mann Whitney U test performed on the difference between control and treatment, *n* is the number of samples involved. $\eta^2$ was used to explain the fraction of the variability in the ranks that can be accounted for by blocking of pipe outlets.

## 5 | RESULTS

### 5.1 | Water budget

The first 12 months from 1 April 2018 were relatively dry, with 844 mm compared to the long-term mean of 1313 mm. Rainfall between 1 April 2019 and 29 February 2020, was more typical with a total of 1467 mm. Summer (JJA), autumn (SON) and winter (DJF) were all considerably wetter in 2019 compared to 2018, with 382, 546 and 376 mm in 2019 versus 121, 266 and 165 mm in 2018 respectively (Figure 4). Rainfall totals were comparable for the period April–May in 2018 and 2019, with 118 mm in 2018, compared to 112 mm in 2019,

**TABLE 2** The number of hydrographs per gauge that met the required criteria for analyses

| | Pre-blocking period | Post-blocking period | Total per gauge |
|---|---|---|---|
| Control catchment | 61 | 35 | 96 |
| Treatment catchment | 59 | 36 | 95 |
| Pipe outlet H1 | 73 | 34 | 107 |
| Pipe outlet H2 | 80 | 16 | 96 |
| Pipe outlet E1 | 64 | - | 64 |
| Pipe outlet E2 | 45 | 17 | 62 |

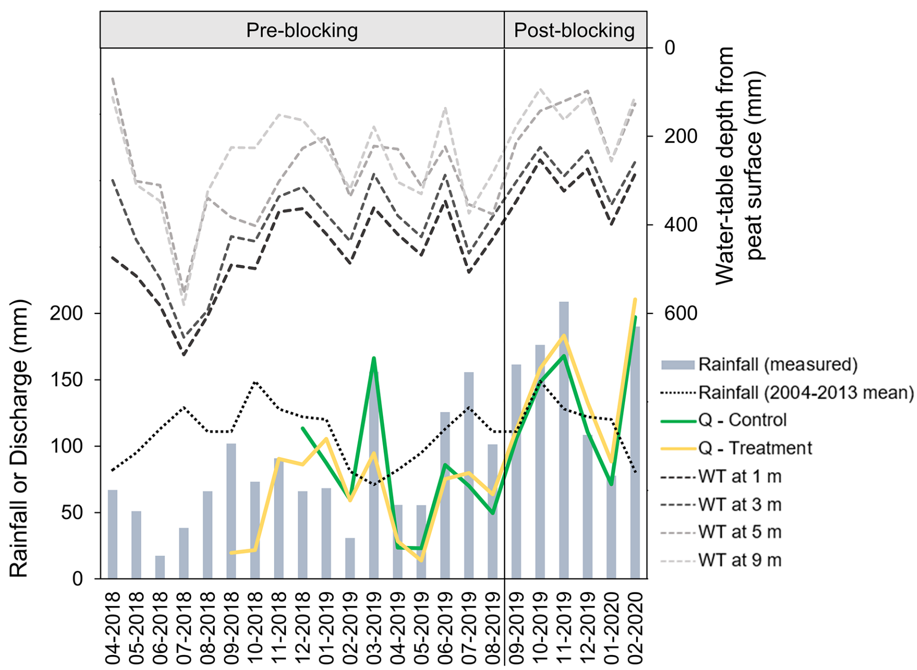


**FIGURE 4** Monthly rainfall over the period April 2018 – February 2020. The mean rainfall between 2004–2013 is shown for reference (based on Clay & Evans, 2017). Total discharge for the control (Q – Control) and treatment catchment (Q – Treatment). Monthly median water-table depths from peat surface (WT) are specified for dipwell positions at 1, 3, 5 and 9 m away from the pipe outlet following transect α (see Figure 3) (grey dashed lines, with increasing shading for increasing distance away from pipe outlet)

respectively. The maximum 15-min rainfall intensity was 35.3 mm h$^{-1}$, recorded on 24 July 2019. Water budgets for the treatment and control catchments were similar to each other from month to month (Figure 4). Over the whole monitoring period, when both stream runoff records were available, the runoff coefficient was 85.9% for the treatment catchment and 85.2% for the control catchment. In winter periods, both sub-catchments show rainfall conversions larger than 100%, which may be due to delayed snow melt events or surface catchment areas not aligning with subsurface catchment areas where piping is an ubiquitous process.

## 5.2 | Success of pipe outlet blocking

Blocked pipe outlets were assessed for leakiness through observations of seepage on 12 occasions between August 2019 and February 2020. Not all pipe outlets could be assessed on each visit, but in total 86 observations were recorded. Seepage around blocked pipe outlets was recorded in 86% of observations. After 25 September 2019, seepage was observed in more than half of the pipe outlets on visit days with an API >10 mm. Seepage was observed at a median of 14 days since blocking. Seepage was observed within 26 days of blocking at pipe outlets plugged with a mixture of peat and stones, as early as 5 days since blocking at wooden plank screens, and as early as the day of blocking at plastic piling screens. Three quarters of all blocked outlets showed signs of seepage within 36 days of blocking. One pipe outlet blocked by a wooden plank only showed the first signs of seepage after 90 days since blocking. The occurrence of leaks was recorded 95% for stone and peat blocks, 83.3% for wooden planks, and 82.9% for plastic pilling (Table 3).

Seepage was observed via the old outlet (57%), new outlets (15.1%), or both (2.3%) (Table 3). Flow from new pipe outlets was observed in 37.5% of pipe outlets blocked by screens of wooden planks and 11.8% of pipe outlets blocked by screens of plastic piling (Table 3). In the majority of the seepage observations, flow rates across blocked pipe outlets were <0.5 L s$^{-1}$, with 36% for <0.05 L s$^{-1}$ and 39.5% for 0.05–0.5 L s$^{-1}$ (Table 3). New outlets occurred within a range of 0.3 to 2.0 m from the original outlet, on both left and right hand sides, and both shallower and deeper than the blocked pipe outlet.

## 5.3 | Storm analyses

### 5.3.1 | Stream responses

The combined effect of pipe outlet blocking on stream responses ranged between 0.014 and 0.207, with medians being significantly different across intervention periods for peak discharge and response index (Figure 5).

The treatment catchment showed increased median runoff coefficients across intervention periods. The control had significantly different distributions of runoff across intervention periods (Table 4, Figure S3). In the post-blocking period, distributions of runoff coefficient were similar between catchments. Median runoff coefficients were significantly different in the pre-blocking period, with the treatment catchment producing much less discharge per mm rainfall compared to the control (Table 4, Figure S3). Peak flows ranged from 0.1 to 16.8 L s$^{-1}$ in the treatment catchment, and 0.1 and 20.1 L s$^{-1}$ in the control catchment. Pipe outlet blocking did not affect differences between treatment and control catchments for peak discharge and peak lag (Table 4). The treatment catchment produced significantly smaller median peak discharges compared to the control catchment in the period before blocking, but peak discharges were the same for both catchments in the post-blocking period (Table 4, Figure S3). Median peak discharges in the post-blocking period were significantly larger compared to those in the pre-blocking period for the treatment catchment, but were the same for the control catchment across intervention periods (Table 4, Figure S3). No significant differences were found between catchments or intervention periods for peak lag ($p$ < 0.05) although the difference of median peak lag for the treatment catchment between intervention periods was marginally significant at $p$ = 0.066 (Table 4). Flow duration was found to be the same in catchments and across intervention periods. Therefore, differences between response indices mimic those of the peak discharge. In the pre-blocking period, hydrograph shapes were significantly different between the treatment catchment and the control catchment, but in the post-blocking period their hydrograph shape was similar (Table 4, Figure S3).

### 5.3.2 | Pipe response

Between 11 September 2018 and 1 September 2019, the four monitored pipe outlets, which were the largest in the treatment catchment,

**TABLE 3** Summary of the leakiness of blocked pipe outlets, detailing the number of observations on (1) flow rate of seepage, and (2) the dominant flow route of seepage (not identifiable, old outlet only, new outlet only, both old and new pipe outlets)

| | Flow rate of seepage (*n*) | | | | Flow route of seepage (*n*) | | | |
|---|---|---|---|---|---|---|---|---|
| Blocking method | No flow | Low (<0.05 L s$^{-1}$) | Medium (0.05–0.5 L s$^{-1}$) | High (>0.5 L s$^{-1}$) | Unidentifiable | Old only | New only | Old + new |
| Stone + Peat (*n* = 6) | 1 | 8 | 8 | 4 | 2 | 18 | 0 | 0 |
| Wooden plank (*n* = 8) | 4 | 5 | 10 | 5 | 0 | 10 | 9 | 1 |
| Plastic piling (*n* = 17) | 7 | 18 | 16 | 0 | 8 | 21 | 4 | 1 |

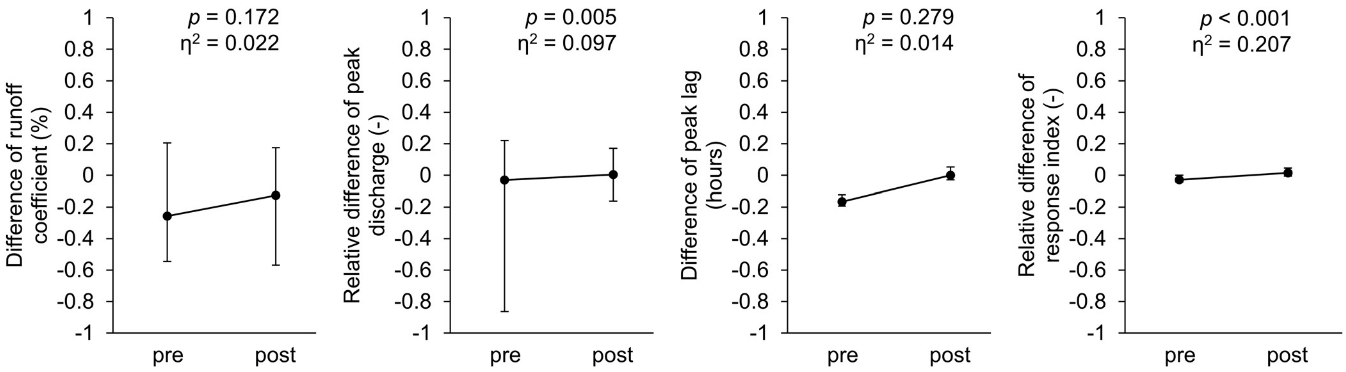


**FIGURE 5** Interaction plots for differences (treatment minus control) before and after pipe outlet blocking for runoff coefficient (%), standardized peak discharge (–), peak lag (hours), and standardized response index (–), calculated for 84 storm responses (pre: 49, post: 35). Positive values on the y-axis indicate that the metric of interest is larger in the treatment catchment than in the control catchment, while negative values indicate the opposite. The whiskers indicate the lowest and highest values that are still within the range: [Q1 – Q2–1.5 * (Q3 - Q1)] and [Q3 - Q2 + 1.5 * (Q3 - Q1)]. For each metric the difference of variation and the statistical response variable $\eta^2$ was determined. Note that the y-axis of the plots may have different scales

**TABLE 4** Statistical analyses of storm responses, providing Mann–Whitney U test results for differences across catchments and monitoring periods with medians for runoff coefficient, peak discharge, peak lag and response index

| | | Differences across catchments | | Differences across Monitoring periods | |
|---|---|---|---|---|---|
| Parameter | Period | *p* - value | N samples | Control ($n$ = 95) | Treatment ($n$ = 94) |
| Runoff coefficient (%) | Pre | 0.005 | 118 | 50.7 | 30.4 |
| | Post | 0.709 | 71 | 68.0 | 66.5 |
| | | | | $p = 0.004$ | $p < 0.001$ |
| Peak discharge (L $s^{-1}$) | Pre | 0.018 | 118 | 5.4 | 3.3 |
| | Post | 0.159 | 71 | 7.7 | 6.7 |
| | | | | $p = 0.104$ | $p = 0.012$ |
| Peak lag (h) | Pre | 0.631 | 118 | 2.0 | 2.4 |
| | Post | 0.881 | 71 | 1.6 | 1.7 |
| | | | | $p = 0.211$ | $p = 0.066$ |
| Response index (L $s^{-2}$) | Pre | 0.014 | 118 | 1111 | 548 |
| | Post | 0.218 | 71 | 1602 | 1127 |
| | | | | $p = 0.524$ | $p = 0.039$ |

contributed 11.3% to storm discharge, with the two head pipes contributing 9.3% (pipe H1: 2.0%, pipe H2: 7.3%) and the two edge pipes 2.0% (pipe E1: 0.7% + pipe E2: 1.3%). In the post-blocking period, 1 September 2019 to 1 March 2020, pipe water that escaped from the blocked pipes contributed 4.3% to stream stormflow (pipe H1: 2.3%, pipe H2: 1.8%, pipe E2: 0.1%). Pre-blocking, a clear differentiation was observed between discharge responses of pipe outlets at head and edge locations, especially when comparing contribution area to API and event rainfall (Figure S4a). Increased dynamic contribution area resulted in a larger peak discharge with a strong relationship for head locations in both intervention periods (Figure S4b). Peak lag was not dependent on dynamic contribution area for both head and edge locations (Figure S4b).

In the pre-blocking period, the distributions of storm discharge between head and edge locations were significantly different ($p < 0.001$, $n = 262$) (Table 5, Figure S4). Pre-blocking, the distributions of storm discharge were significantly different between pipe outlets at head locations (pipe H1 and pipe H2) ($p < 0.001$, $n = 153$) and pipe outlets at edge locations (pipe E1 and pipe E2) ($p < 0.001$, $n = 109$) (Table 5, Figure S5). No evidence indicated that storm discharge was different between pipe H1 and pipe H2 post blocking (Table 5). Median storm discharge increased across intervention periods for pipe H1 ($p = 0.009$, $n = 107$), whereas the opposite was observed for pipe H2 ($p = 0.028$, $n = 96$) (Table 5, Figure S5). No data were available for pipe E1 in the post-blocking period due to instrument failure. Pipe E2 only produced discharge during two of the

**TABLE 5** Comparison of storm pipeflow responses in the pre- and post-blocking period, with median values per metric for each pipe outlet for storm discharge (L), peak lag (h), peak discharge (L $s^{-1}$), dynamic contribution area ($m^2$) and response index (L $s^{-2}$). For each metric Mann–Whitney U test outputs (MWU) at 95% significance interval are indicated for comparisons across intervention period and across pipe outlet location

| | Pre-blocking | *n* | Post-blocking | *n* | MWU |
|---|---|---|---|---|---|
| **Storm discharge (L)** | | | | | |
| Pipe H1 | 714 | 73 | 1670 | 34 | $p = 0.009$ |
| Pipe H2 | 3528 | 80 | 1606 | 16 | $p = 0.028$ |
| MWU | $p < 0.001$ | | $p = 0.618$ | | |
| Pipe E1 | 247 | 64 | No data | - | - |
| Pipe E2 | 943 | 45 | 0 | 17 | $p < 0.001$ |
| MWU | $p < 0.001$ | | - | | |
| **Peak discharge (L $s^{-1}$)** | | | | | |
| Pipe H1 | 0.060 | 72 | 0.108 | 34 | $p = 0.072$ |
| Pipe H2 | 0.220 | 79 | 0.116 | 15 | $p = 0.084$ |
| MWU | $p < 0.001$ | | $p = 0.680$ | | |
| Pipe E1 | 0.018 | 64 | No data | - | - |
| Pipe E2 | 0.069 | 45 | 0.028 | 2 | $p = 0.204$ |
| MWU | $p < 0.001$ | | - | | |
| **Peak lag (h)** | | | | | |
| Pipe H1 | 2.9 | 72 | 2.3 | 34 | $p = 0.164$ |
| Pipe H2 | 2.5 | 79 | 3.2 | 15 | $p = 0.287$ |
| MWU | $p = 0.409$ | | $p = 0.051$ | | |
| Pipe E1 | 2.2 | 64 | No data | - | - |
| Pipe E2 | 2.0 | 45 | −0.1 | 2 | $p = 0.204$ |
| MWU | $p = 0.902$ | | - | | |
| **Dynamic contribution area ($m^2$)** | | | | | |
| Pipe H1 | 156 | 73 | 341 | 34 | $p < 0.001$ |
| Pipe H2 | 673 | 80 | 265 | 16 | $p < 0.001$ |
| MWU | $p < 0.001$ | | $p = 0.092$ | | |
| Pipe E1 | 48 | 64 | No data | - | - |
| Pipe E2 | 144 | 45 | 0 | 17 | $p < 0.001$ |
| MWU | $p < 0.001$ | | - | | |
| **Response index (L $s^{-2}$)** | | | | | |
| Pipe H1 | 16.620 | 72 | 13.196 | 34 | $p = 0.478$ |
| Pipe H2 | 9.569 | 79 | 15.191 | 15 | $p = 0.432$ |
| MWU | $p = 0.037$ | | $p = 0.819$ | | |
| Pipe E1 | 13.072 | 64 | No Data | - | - |
| Pipe E2 | 11.209 | 45 | 20.423 | 2 | $p = 0.599$ |
| MWU | $p = 0.968$ | | - | | |

17 storms after it was blocked. As a result, storm discharge distributions for pipe E2 were significantly different across intervention periods ($p < 0.001$, $n = 62$) (Table 5). Because pipe E2 rarely flowed in the post-blocking period, analyses of peak discharge and peak lag were omitted. As all pipes received a blocking treatment in August 2019, a subset of data comparing the same times of year pre and post blocking were compared (September 2018–February 2019; September 2019–February 2020). Due to limited edge pipe data post-blocking, comparisons between years were only performed for head pipes. Median storm discharge was 2.2 $m^3$ for 2018/19 ($n = 47$) and 1.7 $m^3$ for 2019/20 ($n = 48$). Total storm discharge was 177.9 $m^3$ for 2018/19 and 128.6 $m^3$ for 2019/20. Despite 2018/19 being 26.4% wetter, no evidence was found to indicate that distributions of head pipe storm discharge differed significantly between 2018/19 and 2019/20 ($p = 0.364$, $n = 95$).

In the full pre-blocking period, peak storm discharge for the four monitored pipes ranged from 0.001 to 0.859 L $s^{-1}$. In the same period, distributions of storm peak discharge were significantly different between head and edge locations ($p < 0.001$, $n = 260$) (Table 5, Figure S4), between pipe outlets at head locations (pipe H1 and pipe H2) ($p < 0.001$, $n = 151$), and between pipe outlets at edge locations (pipe E1 and pipe E2) ($p < 0.001$, $n = 109$) (Table 5, Figure S5). Across intervention periods, median storm peak discharges were marginally significantly different for pipe H1 ($p = 0.072$, $n = 106$) and pipe H2 ($p = 0.084$, $n = 94$) (Table 5, Figure S5).

In the pre-blocking period, distributions of dynamic contribution area were significantly different for head and edge locations ($p < 0.001$, $n = 262$) (Table 5, Figure S4). In the pre-blocking period, distributions of dynamic contribution area for pipe H1 and pipe H2 were significantly different ($p < 0.001$, $n = 153$), and for pipe E1 and pipe E2 ($p < 0.001$, $n = 109$) (Table 5, Figure S5). Post-blocking, medians for dynamic contribution area of pipe H1 and pipe H2 were marginally significantly different to each other ($p = 0.092$, $n = 50$) (Table 5, Figure S5). Across intervention periods, a significant difference was found between median dynamic contribution area for pipe H1 ($p < 0.001$, $n = 107$), and distributions of dynamic contribution area for pipe H2 ($p < 0.001$, $n = 96$) (Table 5, Figure S5).

Peak lag was not different between pipes in the pre-blocking period. Post-blocking, median peak lag differed marginally between pipe H1 and H2 ($p = 0.051$, $n = 49$) (Table 5). Peak lag and time from peak flow to baseflow for pipes was the same as for the stream in both intervention periods.

## 5.4 | Water-table responses

Overall, average water table was at its deepest during JJA 2018 and its shallowest during DJF 2018–19 (Figure 4). Mean water-table depth across all monitored dipwells was 364 mm in the pre-blocking period and 247 mm post-blocking. Water-table recession rates over 6 h were distributed significantly differently across intervention periods for pipe H1 ($p = 0.013$, $n = 101$), pipe H2 ($p = 0.030$, $n = 82$)

and were marginally different for pipe E1 ($p = 0.052$, $n = 74$) (Figure S6). Distributions of water-table recession rates over 12 h were significantly different across intervention periods for pipe H1 ($p = 0.005$, $n = 94$), pipe H2 ($p = 0.008$, $n = 78$), and pipe E2 ($p = 0.006$, $n = 90$) (Figure S6).

In the post-blocking period, the lower boundary of the water-table depth at the automated dipwell at pipe H1 stabilized at around 400 mm, but such strong effects were not observed in other dipwells in the vicinity of pipe H1, nor in water-table timeseries at the other pipe outlets (Figure 6).

In both transects β and γ at pipe H1 and pipe E2, median water-table depths were considerably lower and less varied over time at positions not directly above the projected pipe course compared to other pipe outlets (transect α) (Figure S7). At head locations, distributions of water-table depth were significantly different across intervention periods for dipwells at 1 m ($p < 0.001$) and 5 m ($p = 0.003$) from the pipe outlet (Table 6). At head locations, median water-table depth decreased across intervention periods at 3 m ($p = 0.001$) and 9 m ($p = 0.02$) from the pipe outlet (Table 6). At edge locations, median water-table depth decreased significantly across intervention periods at 1, 3 and 5 m from the pipe outlet (Table 6). Dipwells at 9 m from the pipe outlet at edge locations had similar distributions across intervention periods (Table 6). In the pre-blocking period, median water-table depths at dipwells 1 and 9 m from the pipe outlet were significantly shallower for head locations compared to edge locations. Distributions of water-table depths differed significantly between head and edge locations in the pre-blocking period at 3 m from the pipe outlet, and in the post-blocking period at 1, 3 and 9 m from the pipe outlet (Table 6). Water-table depth at 5 m from the pipe outlet was not significantly different between head and edge locations in both intervention periods (Table 6).

Across the whole monitoring period a clear drawdown of the water table was observed along dipwell transect α, with increasing water-table depths towards the pipe outlet. Drawdowns ranged from 94 to 115 mm between 1 and 3 m away from the pipe outlet, and

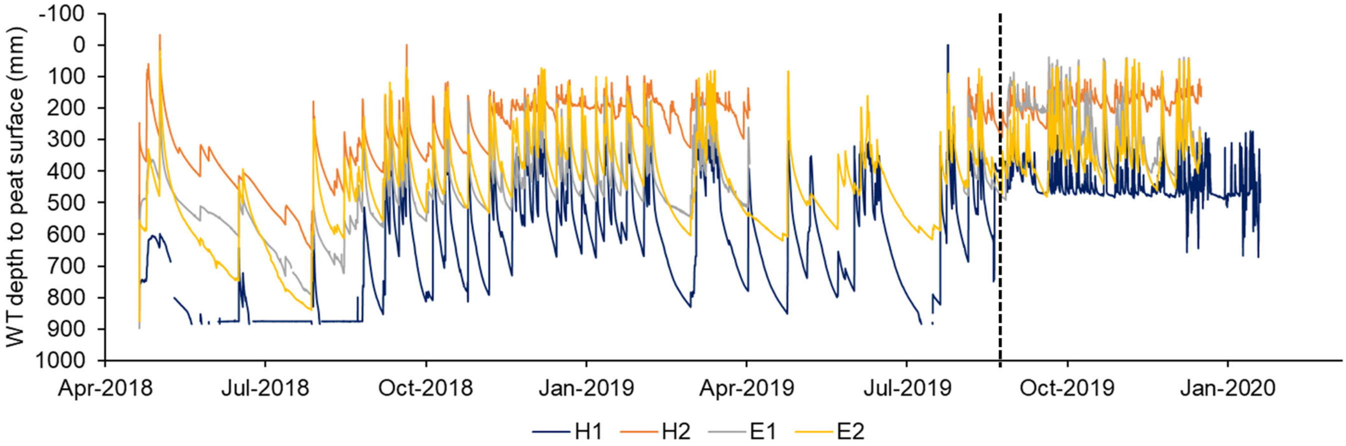


**FIGURE 6** Timeseries of water-table depth at automated dipwell stations for pipes H1, H2, E1 and E2. Vertical dotted line indicated time of blocking pipe outlets

**TABLE 6** Differences in water-table depth relative to the peat surface (mm) at pipe outlet locations (head and edge) at 1, 3, 5, 9 m from the pipe outlet (following transects α, see Figure 3), with median water-table depth for both intervention periods (pre and post), and tests of difference between intervention periods and between head and edge locations

| | | Distance from pipe outlet (m) | | | |
|---|---|---|---|---|---|
| | | 1 | 3 | 5 | 9 |
| Head | Pre-blocking | 407.4 | 300.5 | 268.5 | 200 |
| | Post-blocking | 279.4 | 193.1 | 131 | 94 |
| | $p$-value ($n$ = 68) | < 0.001 | 0.001 | 0.003 | 0.02 |
| Edge | Pre-blocking | 537.4 | 452.8 | 294 | 475 |
| | Post-blocking | 407.6 | 336.1 | 229 | 393.5 |
| | $p$-value ($n$ = 68) | <0.001 | <0.001 | 0.016 | 0.381 |
| Pre-blocking: Head versus Edge | | $p < 0.001$, $n = 100$ | $p < 0.001$, $n = 100$ | $p = 0.238$, $n = 81$ | $p = 0.001$, $n = 78$ |
| Post-blocking: Head versus Edge | | $p = 0.011$, $n = 36$ | $p < 0.001$, $n = 36$ | $p = 0.126$, $n = 36$ | $p = 0.012$, $n = 36$ |

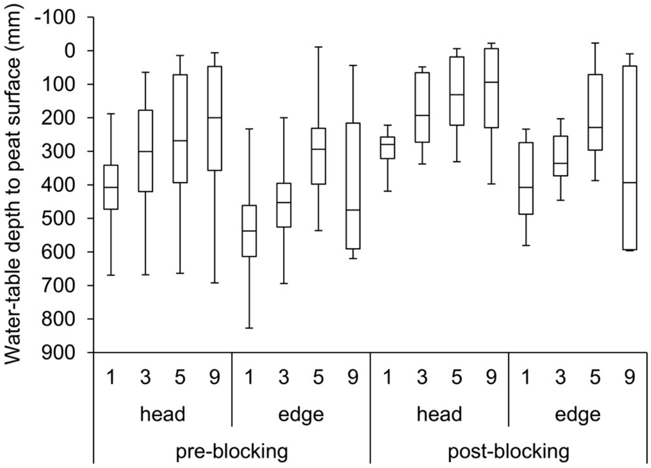


**FIGURE 7** Boxplot of water-table distribution at head and edge locations, across intervention period (pre and post), at 1, 3, 5 and 9 m from the pipe outlet

85 and 156 mm between 3 and 5 m away from the pipe outlet (Figure 7). This distance-decay effect occurred up to 9 m from head pipe outlets and 5 m from edge pipe outlets (Figure 7).

## 6 | DISCUSSION

### 6.1 | Effect of pipe outlet blocking on streamflow

This study assessed, for the first time, the hydrological implications of pipe outlet blocking on streamflow in a heavily degraded blanket bog. Our results show that stormflow responses in two sub-catchments had similar distributions for runoff, peak discharge, peak lag and hydrograph shape after pipe outlets had been blocked in one of them. As shown in Figure 4, the pre-blocking period was drier than the post-blocking period. Storm runoff was the same in both catchments post-blocking, whereas pre-blocking storm runoff in the treatment catchment was 20.3% less than in the control. A similar trend was observed for peak discharge between the two catchments across intervention periods. The increase in storm runoff in the treatment catchment post-blocking may be related to the increased rainfall over the course of the experimental period. A wetter peat profile may promote pipes to drain water from outside the topographic boundary of the catchment, resulting in increased pipe-to-stream runoff contributions in the treatment catchment compared to the control, where fewer pipes were present per catchment area. In addition, the build-up of pipe water behind blocks may have increased hydraulic pressures in the pipe, which has been observed in soil pipes that have clogged naturally (Wanger et al., 2015). In turn, this may have caused surcharging within the pipe network, helping to connect portions of the pipe network that are overflow dependent and that otherwise would not drain below such overflow thresholds (Gilman & Newson, 1980). Pre-blocking, the limited runoff production in the treatment catchment may result from gully blocks in the tributaries, whereas the control only had gully blocks in a small headwater section (see Figure 1c). Gully blocks can provide a reduction in streamflow (Shuttleworth et al., 2019) with impacts most notable in drier conditions when runoff is buffered behind the blocks.

### 6.2 | Success of the different pipe outlet blocking methods

Pipe outlets blocked by either method, insertion of plug-like structures in the pipe-end or the insertion of vertical screens at the pipe outlet perpendicular to the pipeflow direction, showed signs of leakiness. Given that at 75% of the blocked pipes seepage occurred within 6 weeks of blocking, this highlights the challenge in trying to stop pipeflow by blocking outlets. The insertion of plug-like structures into pipe-ends did not result in any reductions of pipeflow as evidenced by flow emerging from pipe outlets post-blocking, but no new exits were observed around pipe outlets blocked by plug-like structures in contrast to pipe outlets blocked by vertical screens.

Laboratory tests by Wanger et al. (2019) showed plugs of compressed sand inserted into pipes mobilized regardless of the pressurized time, particularly when the plugs became saturated. However, the hydraulic conductivity of peat is often very low at depth within the peat profile and so in theory could provide a suitable plug substrate. Nevertheless exposed peat can desiccate and crack. Thus the peat in the trialled plug-like structures may have been exposed to air drying on gully edges, leading to leaks. Insertion and alignment of vertical screens perpendicular to pipe courses was difficult due to local differences in topography and lack of knowledge about the actual pipe course. The screens provided a smooth surface along which accumulated pipe water could flow. This may have increased the propensity to form new pipe outlets. This effect may have been larger for pipe outlets blocked with wooden planks as they were thicker than the plastic pilling and bent more easily when inserted, thereby increasing the width of horizontal incision along which water could flow. However, it should be noted that new pipe outlets may also occur at random and existing ones may become blocked naturally and disappear over time, as the result of the ongoing development of the pipe network (Holden et al., 2012).

### 6.3 | Effect of blocking on pipeflow

Despite all four monitored pipe outlets being ephemeral, they contributed up to 11.3% of streamflow. The largest contribution came from pipe H2 (7.3%), which is relatively high for an individual pipe compared to other studies on ephemeral piping (Chapman et al., 1997), but it should be noted that UNG is still in a phase of active erosion (Evans et al., 2006). Other peatland pipe studies (all northern England blanket peat) showed that the pipe network (both perennial and ephemeral) contributed 9% to 36% of streamflow (Holden et al., 2006; Holden & Burt, 2002; R. P. Smart et al., 2013). The maximum peak discharge from a single peaked hydrograph event in our study was 0.859 L $s^{-1}$ (pipe H1), an order of magnitude smaller than the 9.81 L $s^{-1}$ reported on the largest pipe in the Wye headwaters of mid-Wales (Chapman et al., 1997; Muscutt et al., 1993), and 77% lower than the maximum pipeflow reported from a peatland in northern England (R. P. Smart et al., 2013).

Our results suggest that head pipes produced consistently larger contributions to streamflow compared to pipe outlets at edge locations. Given that head pipes make up 40% of identified pipe outlets in the treatment catchment compared to ~12% in the control (Regensburg, 2020), and 25% of the total identified pipe outlets in the Upper North Grain catchment, the contribution of pipeflow to streamflow in the treatment catchment was probably much larger than that we were able to monitor in this study. This suggests that if practitioners seek to moderate pipe-to-stream connectivity, most effort should be made to impede flow from pipe outlets at head locations. However, the variability in the degree to which individual head pipes responded to blocking underlines the need for further research on factors that control pipeflow.

Despite differences in peak lag not being observed between pipes, volumes of runoff differed markedly across pipe locations and individual pipe outlets. Pipe H2 (head pipe) produced discharge and peak flows one order of magnitude larger than the other three pipes. Also, following pipe outlet blocking, head pipes (pipe H1 and pipe H2) displayed contrasting responses to blocking. For instance, at pipe H1, increases in both dynamic contribution area and peak discharge were observed post-blocking. Such change in flow behaviour may indicate increased connectivity upstream of the pipe outlet within the pipe network and adjacent to the block, due to better utilization of remnant pipe channels that were not previously as frequently connected to the main pipe course. Large dynamic contribution areas may indicate good connectivity between the surface and the pipe network, which may link drought cracks or segments of collapsed pipe roof, forming vent holes. However, such forms of surface-to-pipe network integration were only observed upstream of the outlet of pipe H2 where overland flow was actively infiltrating via vent-holes into the pipe network.

However, post-blocking, the lag time of pipe H2 increased, and its peak flows and dynamic contribution area decreased significantly. The blocking of pipe H2 may have resulted in a backwater effect that forced pipe water back into the pipe network. Return flow can naturally occur in pipes after clogging of the network and may exacerbate internal erosion (Gilman & Newson, 1980). Such return flow may promote the redistribution of pipe water. In turn, blocking pipe outlets may result in a larger spread of pipeflow on gully banks adjacent to the blocked pipe outlets, thereby increasing the propensity of existing pipe networks to further develop inwards (Hagerty, 1991; Parker & Jenne, 1967).

### 6.4 | Water table

The water-table depths at head and edge locations were shallower following pipe outlet blocking across all dipwells. A similar pattern was observed in the water table after subsurface dams were placed perpendicular to an arid gully head, with strong effects locally directly upslope of the barrier (Frankl et al., 2016). Our results showed the water table around pipe outlets to become shallower with increasing distance from the gully edge, but the extent differed between pipe outlet locations both pre- and post-blocking. The distance away from the outlet at which the distance-decay effect was observed appeared to be smaller for edge pipes compared to head pipes. In the same study catchment, Upper North Grain, Allott et al. (2009) observed water tables to drop when closer to the edge of deep gullies (up to 4.5 m), with an effect which extended up to 3.5 m away from the gully edge, measured over 0.5–1.0 m intervals perpendicular to the gully edge. The prevalence of this distance-decay effect was ascribed to the state of degradation of the peat at UNG. Despite streambanks in the treatment catchment only being incised to 2.5 m, they show very similar erosion patterns to those along streambanks investigated by Allott et al. (2009). Such distance-decay effects on the water table were also observed in arid gully systems by Frankl et al. (2016), but they did not report any interactions with pipes. While our water-table data were measured at a spacing of 2 m, the drawdown towards the gully edge was deeper around pipes at edge locations than around head pipes. Surveys of pipe outlets at UNG have shown pipe outlets at edge locations to be deeper in the profile compared to head pipe outlets, and mostly on drier south-facing streambanks (Regensburg et al., 2020). As the hydraulic conductivity of peat decreases with depth in the profile, flow into deep pipe sections may be very small. Therefore, the water table may not be a good reference to pipe connectivity in the gully edge zone. Similar discrepancies between pipe activity and the water table were obtained by Wilson et al. (2017) on soils with fragipans, concluding connectivity based on spatial extent of perched water tables is not always a good indicator of hillslope pipeflow. Consistently deep water tables close to the pipe outlet at those locations would further increase the reach of desiccation and frost heave into deeper layers, which in turn would provide conditions to further promote pipe development by sapping (Parker & Jenne, 1967) and mass movements (Baillie, 1975). Panels E2-$\beta$ and E2-$\gamma$ (Figure S7) show that water table can vary by up to 0.5 m per 1 m lateral distance close to the pipe outlet, and even at 5 m away from the pipe outlet. An absence of water-table inflection across a transect perpendicular to a projected pipe course may be indicative of the difficulty of locating soil pipe position from surface indicators alone (Goulsbra, 2010; Regensburg et al., 2020), which may complicate accurate in-situ blocking practices.

## 7 | CONCLUSIONS AND IMPLICATIONS FOR MANAGERS

Impeding pipeflow by blocking pipe outlets by either plug-like structures in the pipe-end or insertion of a vertical screen at the pipe outlet did not completely prevent all pipeflow. Installing impermeable (wooden and plastic) screens caused new pipe outlets to form, particularly in the degraded gully edge zones where water tables are generally deep. The formation of new pipe outlets as a result of pipe outlet blocking should be considered as an undesirable side effect and therefore be prevented if peatland practitioners aim to overcome pipeflow contributions to the drainage network. Therefore we do not advocate blocking of pipes at the pipe outlet as part of peatland restoration. As blocking of pipe outlets is time consuming and labour intensive, and gullies are susceptible to increased pipe formation, peatland practitioners should consider control measures that reduce pipeflow further upslope of their outlets. Blocking pipes further upslope away from streambanks would generate a return flow which would spill onto the surface via existing desiccation cracks, before following a path through vegetated surfaces with a much lower flow velocity (Grayson et al., 2010; Holden et al., 2008), thereby potentially delivering greater flood benefits than pipe outlet blocking.

Overall, our study assessed the effects of pipe outlet blocking on streamflow, pipeflow, and the water table surrounding pipe outlets. We have shown that permanent blocking of peat pipes has had no direct impact on streamflow. When pipes were active, pipes at head locations contributed more to streamflow compared to pipes at edge locations. Thus, a primary focus should be on pipe outlets at head locations. Pipe blocking at the outlet had a measurable impact on water table but its extent was very localized. Water tables in gully edge zones showed a distance-decay effect, with significantly deeper water tables at edge locations compared to head locations, but a larger reach further away from the gully at head locations. Further work is required to test upslope pipe blocking impacts, away from outlets, to establish if this has greater impacts than the blocking of outlet locations alone. However, more precise mapping of pipe networks will be required, potentially using more recent advances in ground penetrating radar detection so that peat pipes <10 cm in diameter can be mapped (Bernatek-Jakiel & Kondracka, 2019; Holden et al., 2002).

## ACKNOWLEDGEMENTS

The research was jointly funded by EU MOORLIFE2020-D3 awarded to Moors for the Future Partnership and by the School of Geography, University of Leeds. The authors gratefully acknowledge the support of the Peak District National Park Authority, The National Trust, and Natural England for granting site access and permissions. We are extremely grateful to all volunteers that helped construct the monitoring site, field equipment, and helped with data collection. We thank Joseph Margetts for support in volunteer arrangements, David Ashley for field kit construction and on-site troubleshooting, and Philippa Lewis for illustration design. We would like to thank Glenn Wilson and Anita Bernatek-Jakiel for reviewing an earlier version of the paper and for their suggestions to improve the manuscript.

## DATA AVAILABILITY STATEMENT

The data for this paper will be made available on the University of Leeds data repository with a published DoI to be released once the paper is accepted.

## ORCID

*Taco H. Regensburg* https://orcid.org/0000-0002-3935-4063
*Joseph Holden* https://orcid.org/0000-0002-1108-4831

## REFERENCES

Acreman, M., & Holden, J. (2013). How wetlands affect floods. *Wetlands*, *33*(5), 773–786. https://doi.org/10.1007/s13157-013-0473-2

Allott, T. E. H., Evans, M. G., Lindsay, J. B., Agnew, C. T., Freer, J. E., Jones, A., & Parnell, M. (2009). *Water tables in Peak District blanket peatlands*. Retrieved from Edale: https://www.research.manchester.ac.uk/portal/files/38525401/FULL_TEXT.pdf

Anderson, A. E., Weiler, M., Alila, Y., & Hudson, R. O. (2009). Dye staining and excavation of a lateral preferential flow network. *Hydrol. Earth Syst. Sci*, *13*(6), 935–944. https://doi.org/10.5194/hess-13-935-2009

Anderson, M., & Burt, T. P. (1982). Throughflow and pipe monitoring in the humid temperate environment. In R. Bryan & A. Yair (Eds.), *Badland geomorphology and piping* (pp. 337–353). Geo Books.

Baillie, I. C. (1975). Piping as an erosion process in the uplands of Sarawak. *Journal of Tropical Geography*, *41*, 9–15.

Bernatek-Jakiel, A., & Kondracka, M. (2019). Detection of soil pipes using ground penetrating radar. *Remote Sensing*, *11*(16), 1864. https://doi.org/10.3390/rs11161864.

Bernatek-Jakiel, A., & Poesen, J. (2018). Subsurface erosion by soil piping: Significance and research needs. *Earth-Science Reviews*, *185*, 1107–1128. https://doi.org/10.1016/j.earscirev.2018.08.006

Bonn, A., Holden, J., Parnell, M., Worrall, F., Chapman, P. J., C.D. Evans, Termansen, M., Beharry-Borg, N., Acreman, M. C., Rowe, E., Emmett, B., & Tsuchiya, A. (2010). *Ecosystem services of peat – Phase 1*.

Bryan, R., & Yair, A. (1982). *Badland geomorphology and piping*. Geo Books.

Carey, S. K., & Woo, M.-k. (2002). Hydrogeomorphic relations among soil pipes, flow pathways, and soil detachments within a permafrost Hillslope. *Physical Geography*, *23*(2), 95–114. https://doi.org/10.2747/0272-3646.23.2.95

Chapman, P. J. (1994). *Hydrochemical processes influencing episodic stream water chemistry in a small headwater catchment, Plynlimon, mid-Wales* (Unpub. PhD thesis). University of London, London, UK.

Chapman, P. J., Reynolds, B., & Wheater, H. S. (1993). Hydrochemical changes along stormflow pathways in a small moorland headwater catchment in Mid-Wales, UK. *Journal of Hydrology*, *151*(2), 241–265. https://doi.org/10.1016/0022-1694(93)90238-5

Chapman, P. J., Reynolds, B., & Wheater, H. S. (1997). Sources and controls of calcium and magnesium in storm runoff: The role of groundwater and ion exchange reactions along water flowpaths. *Hydrology and Earth System Sciences*, *1*(3), 671–685. https://doi.org/10.5194/hess-1-671-1997

Chappell, N. A. (2010). Soil pipe distribution and hydrological functioning within the humid tropics: A synthesis. *Hydrological Processes*, *24*(12), 1567–1581. https://doi.org/10.1002/hyp.7579

Clay, G. D., & Evans, M. G. (2017). Ten-year meteorological record for an upland research catchment near the summit of Snake Pass in the Peak District, UK. *Weather*, *72*(8), 242–249. https://doi.org/10.1002/wea.2824

Daniels, S. M., Agnew, C. T., Allott, T. E. H., & Evans, M. G. (2008). Water table variability and runoff generation in an eroded peatland, South Pennines, UK. *Journal of Hydrology*, *361*(1), 214–226. https://doi.org/10.1016/j.jhydrol.2008.07.042

Evans, M., & Warburton, J. (2007). *Geomorphology of upland peat: Erosion, form and landscape change* (xviii ed.). Blackwell.

Evans, M., Warburton, J., & Yang, J. (2006). Eroding blanket peat catchments: Global and local implications of upland organic sediment budgets. *Geomorphology*, *79*(1), 45–57. https://doi.org/10.1016/j.geomorph.2005.09.015

Faulkner, H. (2013). Badlands in marl lithologies: A field guide to soil dispersion, subsurface erosion and piping-origin gullies. *CATENA*, *106*, 42–53. https://doi.org/10.1016/j.catena.2012.04.005

Fearing, D. A., Banks, J., Guyetand, S., Monfort Eroles, C., Jefferson, B., Wilson, D., Hillis, P., Campbell, A. T., & Parsons, S. A. (2004).

Combination of ferric and MIEX® for the treatment of a humic rich water. *Water Research*, *38*(10), 2551–2558. https://doi.org/10.1016/j.watres.2004.02.020

Frankl, A., Deckers, J., Moulaert, L., Van Damme, A., Haile, M., Poesen, J., & Nyssen, J. (2016). Integrated solutions for combating gully erosion in areas prone to soil piping: Innovations from the drylands of Northern Ethiopia. *Land Degradation & Development*, *27*(8), 1797–1804. https://doi.org/10.1002/ldr.2301

Gao, J. H., Holden, J., & Kirkby, M. (2016). The impact of land-cover change on flood peaks in peatland basins. *Water Resources Research*, *52*(5), 3477–3492. https://doi.org/10.1002/2015wr017667

Gilman, K., & Newson, M. (1980). *Soil pipes and pipeflow: A hydrological study in upland Wales*. Geo Abstracts.

Goulsbra, C. S. (2010). *Monitoring the connectivity of hydrological pathways in a peatland headwater catchment* (PhD thesis). University of Manchester.

Grayson, R., Holden, J., & Rose, R. (2010). Long-term change in storm hydrographs in response to peatland vegetation change. *Journal of Hydrology*, *389*(3–4), 336–343. https://doi.org/10.1016/j.jhydrol.2010.06.012

Hagerty, D. J. (1991). Piping/Sapping erosion. I: Basic considerations. *Journal of Hydraulic Engineering*, *117*(8), 991–1008. https://doi.org/10.1061/(ASCE)0733-9429(1991)117:8(991)

Holden, J. (2005). Controls of soil pipe frequency in upland blanket peat. *Journal of Geophysical Research-Earth Surface*, *110*, F01002. https://doi.org/10.1029/2004JF000143

Holden, J., & Burt, T. P. (2002). Piping and pipeflow in a deep peat catchment. *CATENA*, *48*(3), 163–199. https://doi.org/10.1016/S0341-8162(01)00189-8

Holden, J., Burt, T. P., & Vilas, M. (2002). Application of ground-penetrating radar to the identification of subsurface piping in blanket peat. *Earth Surface Processes and Landforms*, *27*(3), 235–249. https://doi.org/10.1002/esp.316

Holden, J., Evans, M. G., Burt, T. P., & Horton, M. (2006). Impact of land drainage on peatland hydrology. *Journal of Environmental Quality*, *35*(5), 1764–1778. https://doi.org/10.2134/jeq2005.0477

Holden, J., Kirkby, M. J., Lane, S. N., Milledge, D. G., Brookes, C. J., Holden, V., & McDonald, A. T. (2008). Overland flow velocity and roughness properties in peatlands. *Water Resources Research*, *44*(6), WR006052. https://doi.org/10.1029/2007WR006052

Holden, J., Smart, R. P., Dinsmore, K. J., Baird, A. J., Billett, M. F., & Chapman, P. J. (2012). Morphological change of natural pipe outlets in blanket peat. *Earth Surface Processes and Landforms*, *37*(1), 109–118. https://doi.org/10.1002/esp.2239

Jones, J. A. A. (1971). Soil piping and stream channel initiation. *Water Resources Research*, *7*(3), 602–610. https://doi.org/10.1029/WR007i003p00602

Jones, J. A. A. (1982). Experimental studies of pipe hydrology. In R. B. Bryan & A. Yair (Eds.), *Badlands geomorphology and piping* (pp. 355–370). GeoBooks.

Jones, J. A. A. (1997a). Pipeflow contributing areas and runoff response. *Hydrological Processes*, *11*(1), 35–41.

Jones, J. A. A. (1997b). The role of natural pipeflow in hillslope drainage and erosion: Extrapolating from the Maesnant data. *Physics and Chemistry of the Earth*, *22*(3-4), 303–308. https://doi.org/10.1016/s0079-1946(97)00149-3

Jones, J. A. A., & Crane, F. G. (1984). Pipeflow and pipe erosion in the Maesnant experimental catchment. In T. P. Butt & D. E. Walling (Eds.), *Catchment experiments in fluvial geomorphology* (pp. 55–72). GeoBooks.

Jones, J. A. A., Richardson, J. M., & Jacob, H. J. (1997). Factors controlling the distribution of piping in Britain: A reconnaissance. *Geomorphology*, *20*(3-4), 289–306. https://doi.org/10.1016/S0169-555X(97)00030-5

Kohler, M. A., & Linsley, R. K. (1951). *Predicting the runoff from storm rainfall*. U.S. Dept. of Commerce, Weather Bureau.

Labadz, J. C., Burt, T. P., & Potter, A. W. R. (1991). Sediment yield and delivery in the blanket peat moorlands of the southern Pennines. *Earth Surface Processes and Landforms*, *16*(3), 255–271. https://doi.org/10.1002/esp.3290160306

Midgley, T. L., Fox, G. A., Wilson, G. V., Felice, R., & Heeren, D. (2013). In situ soil pipeflow experiments on contrasting streambank soils. *Transactions of the ASABE*, *56*(2), 479–488.

Muscutt, A. D., Reynolds, B., & Wheater, H. S. (1993). Sources and controls of aluminium in storm runoff from a headwater catchment in Mid-Wales. *Journal of Hydrology*, *142*(1), 409–425. https://doi.org/10.1016/0022-1694(93)90021-Z

Parker, G. G., & Jenne, E. A. (1967). Structural Failure of Western U.S. highways caused by piping. Retrieved from http://onlinepubs.trb.org/Onlinepubs/hrr/1967/203/203-005.pdf

Rapson, G. L., Sykes, M. T., Lee, W. G., Hewitt, A. E., Agnew, A. D. Q., & Wilson, J. B. (2006). Subalpine gully-head ribbon fens of the Lammerlaw and Lammermoor Ranges, Otago, New Zealand. *New Zealand Journal of Botany*, *44*(4), 351–375. https://doi.org/10.1080/0028825X.2006.9513028

Regensburg, T. H. (2020). *Controls on the spatial distribution of natural pipe outlets in heavily degraded blanket peat - dataset*.

Regensburg, T. H., Chapman, P. J., Pilkington, M. G., Chandler, D. M., Evans, M. G., & Holden, J. (2020). Controls on the spatial distribution of natural pipe outlets in heavily degraded blanket peat. *Geomorphology*, *367*, 107322. https://doi.org/10.1016/j.geomorph.2020.107322

Roberge, J., & Plamondon, A. P. (1987). Snowmelt runoff pathways in a boreal forest hillslope, the role of pipe throughflow. *Journal of Hydrology*, *95*(1), 39–54. https://doi.org/10.1016/0022-1694(87)90114-4

Shuttleworth, E. L., Evans, M. G., Pilkington, M., Spencer, T., Walker, J., Milledge, D., & Allott, T. E. H. (2019). Restoration of blanket peat moorland delays stormflow from hillslopes and reduces peak discharge. *Journal of Hydrology X*, *2*, 100006. https://doi.org/10.1016/j.hydroa.2018.100006

Smart, R. P., Holden, J., Dinsmore, K. J., Baird, A. J., Billett, M. F., Chapman, P. J., & Grayson, R. (2013). The dynamics of natural pipe hydrological behaviour in blanket peat. *Hydrological Processes*, *27*(11), 1523–1534. https://doi.org/10.1002/hyp.9242

Smart, S. M., Henrys, P. A., Scott, W. A., Hall, J. R., Evans, C. D., Crowe, A., Rowe, E. C., Dragosits, U., Page, T., Whyatt, D., Sowerby, A., & Clark, J. M. (2010). Impacts of pollution and climate change on ombrotrophic Sphagnum species in the UK: Analysis of uncertainties in two empirical niche models. *Climate Research*, *45*, 163–176.

Van der Wal, R., Bonn, A., Monteith, D., Reed, M., Blackstock, K., Hanley, N.,, Thompson, D., Evans, M., Alonso, I, Allott, T., Armitage, H., Beharry, N., Glass, J., Johnson, S., McMorrow, J., Ross, L., Pakeman, R., Perry, S., and Tinch, D. (2011). *Mountains, moorlands and heaths*. UK National Ecosystem Assessment. Cambridge, England.

Verachtert, E., Van Den Eeckhaut, M., Poesen, J., & Deckers, J. (2010). Factors controlling the spatial distribution of soil piping erosion on loess-derived soils: A case study from central Belgium. *Geomorphology*, *118*(3), 339–348. https://doi.org/10.1016/j.geomorph.2010.02.001

Wanger, M., Fox, G. A., Wilson, G. V., & Nieber, J. (2019). Laboratory experiments on the removal of soil plugs during soil piping and internal erosion. *Transactions of the ASABE*, *62*(1), 83–93. https://doi.org/10.13031/trans.13092

Wanger, M. M., Fox, G. A., & Wilson, G. V. (2015). *Pipeflow experiments to quantify pore-water pressure buildup due to pipe clogging*. Paper presented at the 2015 ASABE Annual International Meeting, St. Joseph, MI. https://elibrary.asabe.org/abstract.asp?aid=45749&t=5

Ward, S. E., Bardgett, R. D., McNamara, N. P., Adamson, J. K., & Ostle, N. J. (2007). Long-term consequences of grazing and burning on northern peatland carbon dynamics. *Ecosystems*, *10*(7), 1069–1083. https://doi.org/10.1007/s10021-007-9080-5

Wilson, G. (2011). Understanding soil-pipe flow and its role in ephemeral gully erosion. *Hydrological Processes*, *25*(15), 2354–2364. https://doi.org/10.1002/hyp.7998

Wilson, G. V., & Fox, G. A. (2013). Pore-water pressures associated with clogging of soil pipes: Numerical analysis of laboratory experiments.

*Soil Science Society of America Journal*, *77*(4), 1168–1181. https://doi.org/10.2136/sssaj2012.0416

Wilson, G. V., Nieber, J. L., Fox, G. A., Dabney, S. M., Ursic, M., & Rigby, J. R. (2017). Hydrologic connectivity and threshold behavior of hillslopes with fragipans and soil pipe networks. *Hydrological Processes*, *31*, 2477–2496. https://doi.org/10.1002/hyp.11212

Wolverson Cope, F. (1998). *Geology explained in the peak district* (2nd Revised ed.). Scarthin Books.

Xu, J., Morris, P. J., Liu, J., & Holden, J. (2018). Hotspots of peatland-derived potable water use identified by global analysis. *Nature Sustainability*, *1*(5), 246–253. https://doi.org/10.1038/s41893-018-0064-6

Xu, X., Wilson, G. V., Zheng, F., & Tang, Q. (2020). The role of soil pipe and pipeflow in headcut migration processes in loessic soils. *Earth Surface Processes and Landforms*, *45*(8), 1749–1763. https://doi.org/10.1002/esp.4843

Yeloff, D. E., Labadz, J. C., & Hunt, C. O. (2006). Causes of degradation and erosion of a blanket mire in the southern Pennines, UK. *Mires and Peat*, *1*(4), 1–18.

Zhu, T. X., Luk, S. H., & Cai, Q. G. (2002). Tunnel erosion and sediment production in the hilly loess region, North China. *Journal of Hydrology*, *257*(1), 78–90. https://doi.org/10.1016/S0022-1694(01)00544-3

## SUPPORTING INFORMATION

Additional supporting information may be found online in the Supporting Information section at the end of this article.

**How to cite this article:** Regensburg TH, Chapman PJ, Pilkington MG, Chandler DM, Evans MG, Holden J. Effects of pipe outlet blocking on hydrological functioning in a degraded blanket peatland. *Hydrological Processes*. 2021;35:e14102. https://doi.org/10.1002/hyp.14102